Dynamics of an Inertially Driven Robot

Paweł FRITZKOWSKI
Institute of Applied Mechanics, Poznan University of Technology, ul. Jana Pawła II 24, 60-965 Poznan, pawel.fritzkowski@put.poznan.pl

Roman STAROSTA
Institute of Applied Mechanics, Poznan University of Technology, ul. Jana Pawła II 24, 60-965 Poznan, roman.starosta@put.poznan.pl

Abstract

An inertially-driven system that slides on a rough horizontal plane due to periodic oscillations of two internal bodies is studied. Three-phase internal motions with piecewise-constant relative accelerations are considered. It is shown that an always forward motion of the robot can be achieved. The effect of the model parameters on the displacement and average velocity of the system is analyzed.

Keywords: motion control, movable internal mass, vibration-driven robot

1. Introduction

Mobile robots without any external moving parts (like legs, wheels, tracks etc.) have drawn attention of many researchers in recent years. Within this category, a body that can slide on a rough surface due to oscillatory internal motions is perhaps the most curious conception. Such a robot can be imagined as a box containing one or several masses which perform oscillations and interact with the primary body. The internal (relative) motions, rectilinear or rotational, can be controlled to push the entire system in the desired direction. More precisely, the idea is to produce certain inertia forces in order to control the normal force of the robot on the ground (and hence the friction force) as well as the force that tends to displace the box. Thus, systems of this type are called vibration-driven or inertially driven robots.

The absence of outer movers makes the systems relatively simple in design. This feature creates promising possibilities for use in practical applications. For example, one can more easily produce a robot of very small size (micro-robot), or provide a complete enclosure (waterproof, leak-protected etc.) for the robot.

Most papers devoted to vibration-driven systems are focused on optimization of the robot motion (e.g. its average velocity) with respect to parameters of the internal vibrations. Systems moving along a horizontal straight line, having a single internal body, were investigated by Chernous'ko [2, 3]. Fang and Xu analyzed the same robot immersed in a resistive medium [4], and a system of two identical, coupled modules [5]. Figurina [6] considered the optimization problem for the rectilinear motion of a robot up an inclined plane. Dynamics of a system containing two internal masses, moving horizontally or vertically, was analyzed by Bolotnik et. al [1]. Experimental studies of systems containing unbalanced rotors were presented by Sobolev and Sorokin [7].

This paper is devoted to an inertially-driven system that slides on a rough horizontal plane due to periodic oscillations of two internal bodies: one of them moves horizontally, the other vertically. Three-phase internal motions are considered, where the relative accelerations are piecewise-constant. The objective of the studies is to analyze the effect of the model parameters on the displacement and velocity of the robot, and to access efficiency of the proposed, relatively simple conception in comparison with the ideas provided in literature.

2. Mathematical model

Consider a system that consists of a carrying body (box, primary body) of mass M and two internal particles of mass m_1 and m_2 (see Fig. 1). The former one lies on a horizontal plane and can move along the global x axis. The interaction between the box and the ground is characterized by the dry friction coefficient, μ. The internal bodies can move horizontally or vertically under the action of driving control forces F_1 and F_2. The particles interact with the box, e.g. they slide along guide bars rigidly attached to the carrying body. The relative motions are described using the local reference frames fixed to the box: x_1y_1 and x_2y_2.

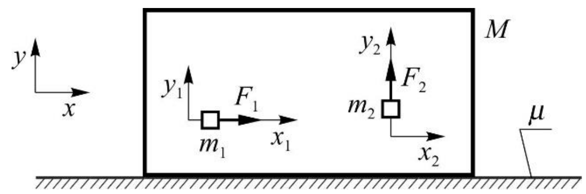

Figure 1. The carrying body with movable internal particles

Let x denote the displacement of the whole mechanical system. For the internal bodies, equations of the horizontal and vertical motion in the inertial frame take the form:

$$m_1(\ddot{x} + \ddot{x}_1) = F_1 , \qquad m_2 \ddot{y}_2 = F_2 . \tag{1}$$

The absolute motion of the system, in turn, is described by

$$(M + m_2)\ddot{x} = -F_1 - F_{\mathrm{fr}} , \tag{2}$$

where F_{fr} is the dry (Coulomb) friction force. Moreover, one can write the following equilibrium equation related to the y direction:

$$(M + m_1)g + F_2 = N , \tag{3}$$

where N denotes the normal component of the ground reaction. Obviously, this normal force is involved in the friction law:

$$F_{\mathrm{fr}} = \begin{cases} F_{\mathrm{fr}}^{(\mathrm{k})} \operatorname{sgn} \dot{x}, & \text{if } \dot{x} \neq 0 \\ F_{\mathrm{int}} , & \text{if } \dot{x} = 0 \text{ and } |F_{\mathrm{int}}| \le F_{\mathrm{fr}}^{(\mathrm{k})} \\ F_{\mathrm{fr}}^{(\mathrm{k})} \operatorname{sgn} F_{\mathrm{int}} , & \text{if } \dot{x} = 0 \text{ and } |F_{\mathrm{int}}| > F_{\mathrm{fr}}^{(\mathrm{k})} \end{cases} \tag{4}$$

In the above formula, $F_{\mathrm{fr}}^{(\mathrm{k})}$ denotes the kinetic friction force while F_{int} is the resultant of all internal (inertial) forces:

$$F_{\mathrm{fr}}^{(\mathrm{k})} = \mu N \,, \tag{5}$$

$$F_{\mathrm{int}} = -[m_1(\ddot{x} + \ddot{x}_1) + m_2\ddot{x}] \,, \tag{6}$$

Assume that the relative accelerations of the particles are known functions of time: $\ddot{x}_1 = a_1(t)$, $\ddot{y}_2 = a_2(t)$. Using Eqs. (1), one can write equation of motion (2) as

$$m_s\ddot{x} = -m_1 a_1 - F_{\mathrm{fr}} \,, \tag{7}$$

where $m_s = M + m_1 + m_2$ is the total mass of the system. Substituting Eqs. (1) and (3) into relation (5) leads to

$$F_{\mathrm{fr}}^{(\mathrm{k})} = \mu(m_s g + m_2 a_2) \,. \tag{8}$$

When it comes to force F_{int}, taking into account the discussion presented in Ref. [1], formula (6) can be replaced with the simpler one:

$$F_{\mathrm{int}} = -m_1 a_1 \,. \tag{9}$$

Thus, the robot motion is described by Eq. (7), where the friction force is determined by (4) together with (8) and (9).

Let us introduce the dimensionless time and displacements:

$$t^* = \frac{t}{T_e}\,, \qquad X = \frac{x}{T_e^2 g}\,, \qquad u_x = \frac{x_1}{T_e^2 g}\,, \qquad u_y = \frac{y_2}{T_e^2 g}\,, \tag{10}$$

where T_e is a characteristic time (some interval length) of the excitation function $a_1(t)$. Consequently, one obtains the non-dimensional form of the equation of motion:

$$\ddot{X} = -\alpha_1 a_x - f_{\mathrm{fr}} \,, \tag{11}$$

where

$$f_{\mathrm{fr}} = \begin{cases} f_{\mathrm{fr}}^{(\mathrm{k})} \operatorname{sgn} \dot{X}, & \text{if } \dot{X} \neq 0 \\ f_{\mathrm{int}}, & \text{if } \dot{X} = 0 \text{ and } |f_{\mathrm{int}}| \leq f_{\mathrm{fr}}^{(\mathrm{k})} \\ f_{\mathrm{fr}}^{(\mathrm{k})} \operatorname{sgn} f_{\mathrm{int}}, & \text{if } \dot{X} = 0 \text{ and } |f_{\mathrm{int}}| > f_{\mathrm{fr}}^{(\mathrm{k})} \end{cases} \tag{12}$$

and

$$f_{\mathrm{fr}}^{(\mathrm{k})} = \mu(1 + \alpha_2 a_y)\,, \qquad f_{\mathrm{int}} = -\alpha_1 a_x \,, \tag{13}$$

$$\alpha_1 = m_1 / m_s\,, \qquad \alpha_2 = m_2 / m_s\,, \qquad a_x = \ddot{u}_x = a_1 / g\,, \qquad a_y = \ddot{u}_y = a_2 / g\,. \tag{14}$$

Obviously, now an overdot denotes the derivative with respect to the dimensionless time t^* (the asterisk will be omitted in further considerations).

3. Internal three-phase motions

We restrict our attention to one of the simplest scenarios for the relative motions of the particles, i.e. periodic three-phase oscillations. Let T denote the oscillation period, while $v_x = \dot{u}_x$, $v_y = \dot{u}_y$. First, consider the horizontal motion. For practical reasons, we impose the conditions: $u_x(0) = u_x(T) = 0$ and $v_x(0) = v_x(T) = 0$. Moreover, the period includes three intervals of constant relative acceleration. Denoting the interval duration by Δt_i (i = 1, 2, 3) and the characteristic time points by $t_i = t_{i-1} + \Delta t_i$ (in particular $t_0 = 0$, $t_3 = T$), we assume the excitation function in the following form:

$$a_x(t) = \begin{cases} a_{x1} & \text{for} \quad 0 \le t < t_1 \\ a_{x2} & \text{for} \quad t_1 \le t < t_2 \\ a_{x3} & \text{for} \quad t_2 \le t < t_3 \end{cases} \tag{15}$$

where a_{xi} are real constants. Consequently, the relative velocity and displacement are piecewise-linear and piecewise-parabolic, respectively (see Fig. 2).

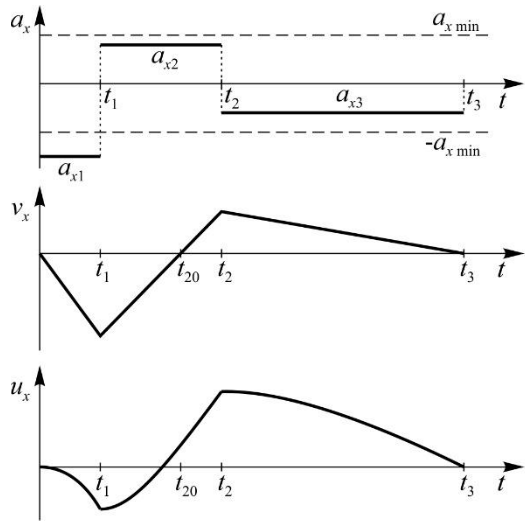

Figure 2. Relative acceleration, velocity and displacement of the internal mass over one period

Consider the system at rest: $X = \dot{X} = 0$. According to Eq. (12), motion of the carrying body can be excited by the first particle if $|f_{\text{int}}| > f_{\text{fr}}^{(\text{k})}$, i.e.

$$|a_x| > \mu \frac{1 + \alpha_2 a_y}{\alpha_1} = a_{x\,\min} \tag{16}$$

Now, the acceleration values for each subinterval are defined as

$$a_{x1} = -c_{x1} a_{x\,\min}, \quad a_{x2} = c_{x2} a_{x\,\min}, \quad a_{x3} = -c_{x3} a_{x\,\min}, \tag{17}$$

where c_{xi} are positive coefficients. In the initial phase $c_{x1} > 1$, which leads to motion of the box to the right (active phase). Next, to avoid its backward motion, it is necessary to take $c_{x2} < 1$. With this assumption, it is impossible to obtain both zero velocity and displacement. Velocity v_x reaches zero for

$$\Delta t_{20} = t_{20} - t_1 = \Delta t_1 \sqrt{\frac{c_{x1}}{c_{x2}}}, \tag{18}$$

hence the second phase duration time is $\Delta t_2 = c_{t2} \Delta t_{20}$, where $c_{t2} > 1$. The third indispensable stage is usually also a rest phase of the box, i.e. $c_{x3} < 1$, and the following relation holds: $\Delta t_1 < \Delta t_2 < \Delta t_3$.

When it comes to the vertical internal motion, the relative acceleration is constrained via the condition of the constant contact between the box and the ground ($N \geq 0$). Taking into account (5) and (13), one can obtain

$$a_y \geq -\frac{1}{\alpha_2} = a_{y\,\min} \tag{19}$$

Now, the acceleration values for each subinterval Δt_i are given by

$$a_{y1} = -a_{y0}, \quad a_{y2} = c_y a_{x2}, \quad a_{y3} = c_y a_{x3}, \tag{20}$$

where $a_{y0} > a_{y\,\min}$ is the base value, and $c_y = a_{y1}/a_{x1}$. Thus, the vertical and horizontal accelerations are proportional, and the dependency $a_y(t)$ is similar to the one shown in Fig. 2.

The conditions of zero relative velocity and zero relative displacement at the end of a period lead to

$$a_{x1} \Delta t_1 + a_{x2} \Delta t_2 + a_{x3} \Delta t_3 = 0 \tag{21}$$

$$a_{x1} \frac{\Delta t_1^2}{2} + a_{x2} \frac{\Delta t_2^2}{2} + a_{x3} \frac{\Delta t_3^2}{2} = 0 \tag{22}$$

This system of equations allows one to determine two parameters, while the others are assumed to be constant.

4. Numerical results

Let us start with numerical solutions of Eq. (11) for selected values of the model parameters. The basic data set is as follows:

$$\mu = 0.1, \ \alpha_1 = \alpha_2 = 0.15, \ c_{x1} = 2, \ c_{x2} = 0.9, \ a_{y0} = 0.1, \ \Delta t_1 = 1, \ c_{t2} = 1.8. \tag{23}$$

Hence $a_{x\,\min} \approx 0.66$ and $a_{y\,\min} \approx -6.67$. The acceleration and duration time of the third phase have been determined as the solution of system (21)-(22): $a_{x3} \approx -0.025$ (which means $c_{x3} \approx 0.038$), $\Delta t_3 \approx 10.8$. For such values of the model parameters, the horizontal relative displacement and velocity over two periods as well as the resulting displacement and velocity of the whole system are shown in Fig. 3. As can be seen, there is a relatively short interval of the box forward motion (active phase), which is followed by a much longer rest phase. A closer look at the graphs indicates that the peak-shape velocity of the system reaches zero at the beginning of the second phase of the internal motions. Moreover, u_x is around ten times larger than X.

The effect of particular parameters on the carrying body motion can be assessed via the total displacement and the average velocity. Assume that the motion occurs without sticking. Direct integration of Eq. (11) over Δt_1 and Δt_2 allows one to estimate the duration of the active phase. Next, the total displacement per period is approximated by

$$X_T = X(T) = \frac{(\mu + \alpha_1 a_{x1} + \mu\alpha_2 a_{y1})}{2(\mu + \alpha_1 a_{x2} + \mu\alpha_2 a_{y2})}[\alpha_1(a_{x1} - a_{x2}) + \mu\alpha_2(a_{y1} - a_{y2})], \tag{24}$$

and the average velocity is $V = X_T/T$. For data set (23) one obtains $X_T \approx 0.075$, $V \approx 0.005$.

Filled contour plots of the total displacement (scaled by a factor of 10^2) on the parameter planes (c_{x1}, c_{x2}) and (c_{x1}, a_{y0}) are presented in Fig. 4; the other parameters take the values (23). The effect of coefficient c_{x1} on X_T is much greater than that of c_{x2}. Generally, X_T increases with increasing c_{x1} and decreasing a_{y0}.

Obviously, the average velocity is a better measure of the robot driving efficiency. By analogy to Fig. 4, maps of V (scaled by a factor of 10^3) are shown in Fig. 5a, b. Unlike for the displacement, both c_{x1} and c_{x2} affect the velocity strongly; the values from the basic data set are related to a quite high velocity zone. When it comes to a_{y0}, its decrease produces an increase in V; it is even advantageous to change its sign (antiphase internal motions). Additionally, the parameter planes (c_{x1}, c_{t2}) and (c_{t2}, a_{y0}) are taken into account in Fig. 5c, d. Compared to c_{x1}, coefficient c_{t2} has a weaker effect on V. Nevertheless, based on the graphs it is possible to select such values of the parameters that maximize the average velocity.

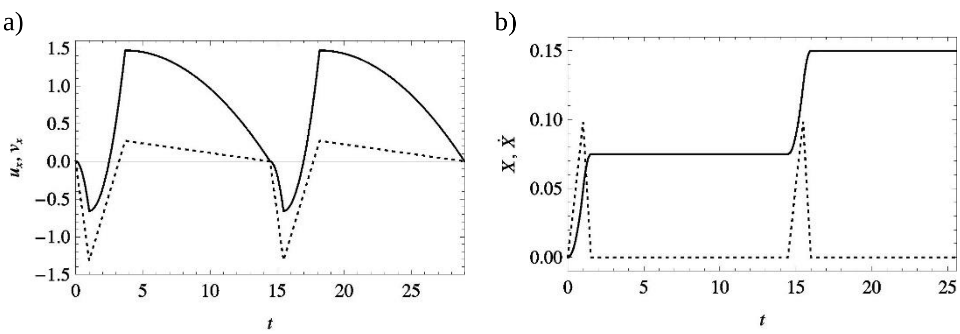

Figure 3. Results for the sample data: a) relative displacement (solid) and velocity (dotted) of the internal mass, b) displacement (solid) and velocity (dotted) of the box

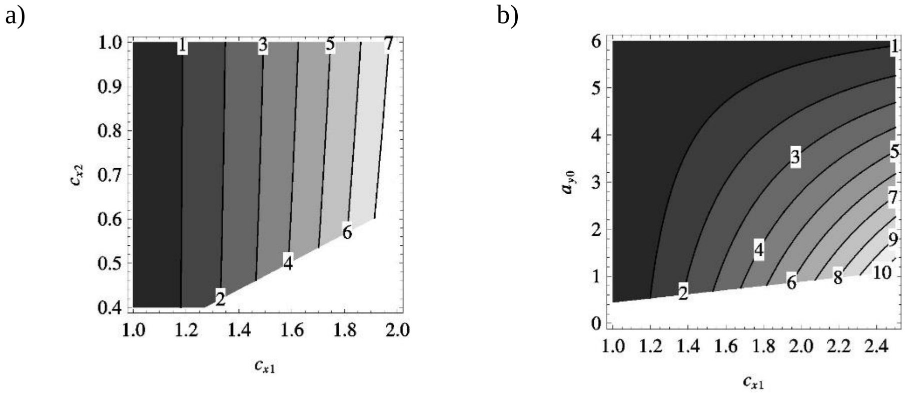

Figure 4. The total displacement $X_T \times 10^2$ for varying parameters:
a) c_{x1} and c_{x2}; b) c_{x1} and a_{y0}

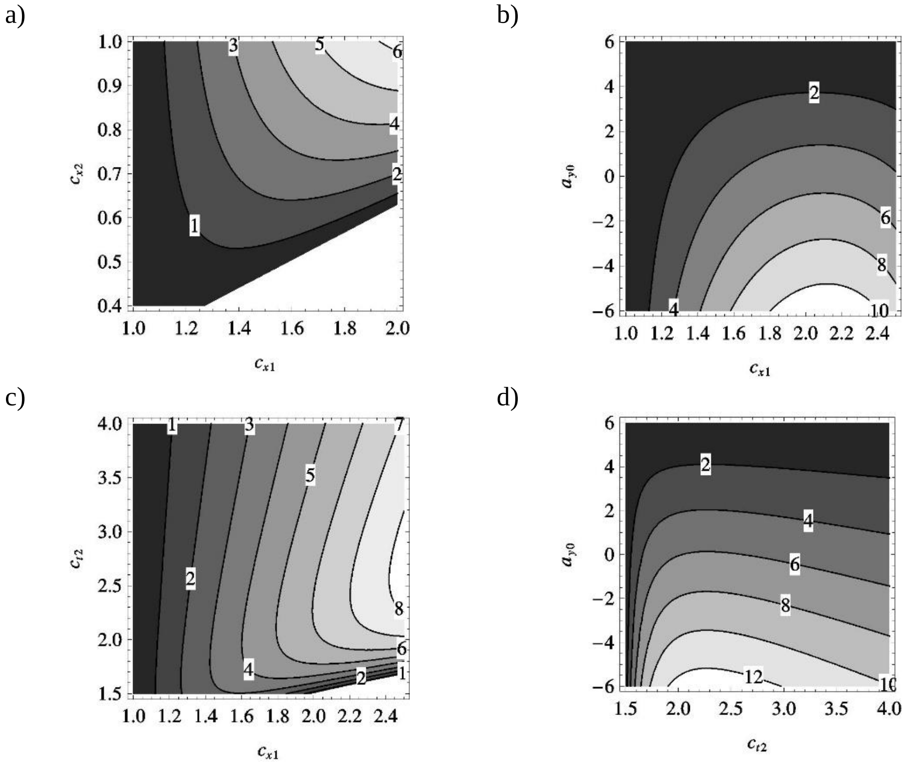

Figure 5. The average velocity $V \times 10^3$ for varying parameters:
a) c_{x1} and c_{x2}; b) c_{x1} and a_{y0}; c) c_{x1} and c_{t2}; d) c_{t2} and a_{y0}

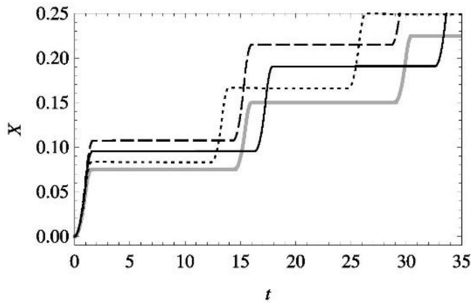

Figure 6. Displacement of the carrying body: the basic data (grey solid);
c_{x1} = 2.1, a_{y0} = -0.5 (solid); c_{x1} = 2.3, c_{t2} = 2.4 (dashed); c_{t2} = 2.4, a_{y0} = -0.5 (dotted)

Figure 6 includes several numerical solutions of the equation of motion obtained for modified values of particular parameters. The reference $X(t)$ dependence (from Fig. 3b) is marked in grey. The black curves correspond to certain changes made on the basis of the contour plots in Fig. 5b-d. In all these cases, the jump in $X(t)$ is greater than for the reference data set. It should be emphasized that, even theoretically, parameter a_{y0} cannot be decreased without bounds. Apart from constraint (19), condition (16) must be fulfilled only in the first phase of the internal motion, according to the assumptions. However, considerable negative values of a_{y0} make the second phase to be active, i.e. the backward motion of the box occurs, and estimation (24) is no longer valid.

5. Conclusions

The discussed conception of the inertially-driven system is relatively simple. As a result of rectilinear periodic oscillations of two internal particles, an always forward motion of the carrying body can be achieved. The active phase is rather short, but a careful selection of the internal motions' parameters allows one to maximize the average velocity of the robot.

Most of the vibration-driven systems analyzed in literature involve unbalance vibration exciters. Actually, it is one of the simplest methods to excite harmonic oscillations. However, such an approach leads to both forward and backward motion of the carrying body, and various control strategies must be used to minimize the effect [1, 4, 5].

From a practical point of view, further studies should incorporate some constraints imposed on the relative displacement, velocity or acceleration of the internal particles, e.g. due to limited dimensions of the carrying body.

Acknowledgments

This work was supported by grants of the Ministry of Science and Higher Education in Poland: 02/21/DS-PB/3513/2018.

References

1. N. N. Bolotnik, I. M. Zeidis, K. Zimmermann, S. F. Yatsun, *Dynamics of controlled motion of vibration-driven systems*, J. Comput. Sys. Sc. Int., **45** (2006) 831 – 840.
2. F. L. Chernous'ko, *On the motion of a body containing a movable internal mass*, Doklady Physics, **50** (2005) 593 – 597.
3. F. L. Chernous'ko, *Analysis and optimization of the motion of a body controlled by means of a movable internal mass*, J. Appl. Math. Mech. – USS, **70** (2006) 819 – 842.
4. H.-B. Fang, J. Xu, *Dynamics of a mobile system with an internal acceleration-controlled mass in a resistive medium*, J. Sound Vibr., **330** (2011) 4002 – 4018.
5. H.-B. Fang, J. Xu, *Controlled motion of a two-module vibration-driven system induced by internal acceleration-controlled masses*, Arch. Appl. Mech., **82** (2012) 461 – 477.
6. T. Yu. Figurina, *Optimal motion control for a system of two bodies on a straight line*, J. Comput. Sys. Sc. Int., **46** (2007) 227 – 233.
7. N. A. Sobolev, K. S. Sorokin, *Experimental investigation of a model of a vibration-driven robot with rotating masses*, J. Comput. Sys. Sc. Int., **46** (2007) 826 – 835.